Drug-polymer interactions in acetaminophen / hydroxypropylmethylcellulose acetyl succinate amorphous solid dispersions revealed by multidimensional multinuclear solid-state NMR spectroscopy

Andrea Pugliese[a], Michael Toresco[b], Daniel McNamara[c], Dinu Iuga[d], Anuji Abraham[c], Michael Tobyn[e], Lucy E. Hawarden[e], and Frédéric Blanc[a,f,*]

[a] *Department of Chemistry, University of Liverpool, Crown Street, Liverpool L69 7ZD, United Kingdom*

[b] *Rowan College of Engineering, Chemical Engineering Department, Rowan University, Mullica Hill Road, Glassboro, New Jersey 08028, United States*

[c] *Drug Product Development, Bristol-Myers Squibb, One Squibb Drive, New Brunswick, New Jersey 08903, United States*

[d] *Department of Physics, University of Warwick, Gibbet Hill Road, Coventry CV4 7AL, United Kingdom*

[e] *Drug Product Development, Bristol-Myers Squibb, Reeds Lane, Moreton CH46 1QW, United Kingdom*

[f] *Stephenson Institute for Renewable Energy, University of Liverpool, Peach Street, Liverpool L69 7ZF, United Kingdom*

* Email: frederic.blanc@liverpool.ac.uk

Supporting Information Placeholder

ABSTRACT: The bioavailability of insoluble crystalline active pharmaceutical ingredients (APIs) can be enhanced by formulation as amorphous solid dispersions (ASDs). One of the key factors of ASD stabilisation is the formation of drug - polymer interactions at the molecular level. Here, we used a range of multidimensional and multinuclear nuclear magnetic resonance (NMR) experiments to identify these interactions in amorphous acetaminophen (paracetamol)/ hydroxypropylmethylcellulose acetyl succinate (HPMC-AS) ASDs at various drug loadings. At low drug loading (< 20% wt.), we showed that ^{1}H-^{13}C through-space heteronuclear correlation experiments identify proximity between aromatic protons in acetaminophen with cellulose backbone protons in HPMC-AS. We also show that ^{14}N-^{1}H heteronuclear multiple quantum coherence (HMQC) experiments are a powerful approach in probing spatial interactions in amorphous materials and establish the presence of hydrogen bonds (H-bond) between the amide nitrogen of acetaminophen with the cellulose ring methyl protons in these ASDs. In contrast, at higher drug loading (40% wt.), no acetaminophen – HPMC-AS spatial proximity was identified and domains of recrystallisation of amorphous acetaminophen into its crystalline form I, the most thermodynamically stable polymorph, and form II are identified. These results provide atomic scale understanding of the interactions in the acetaminophen / HPMC-AS ASD occurring via H-bond interactions.

KEYWORDS: Acetaminophen (paracetamol), Hydroxypropylmethylcellulose acetyl succinate (HPMC-AS), Amorphous solid dispersion, Solid-state NMR, Drug-polymer interactions, Multidimensional NMR.

1 Introduction

Biopharmaceutical Class II active pharmaceutical ingredients (APIs) (or drugs) exhibit poor bioavailability as a result of low aqueous solubility, accompanied by high biological membrane permeability.[1] API can exist either in the crystalline form, characterised by a three-dimensional structure in which molecules are packed in a regularly ordered repeating pattern, or amorphous form defined as an ensemble of molecules/units arranged randomly. The energy barrier required to break down the long-range structure means that crystalline systems can show low solubility, and a low kinetic rate of dissolution. In amorphous systems the lack of long range order greatly enhances the apparent solubility and rate of dissolution.[2] From a thermodynamic view point, the crystalline state is low energy and stable in contrast to the amorphous state which is marked as high energy and unstable. The metastable nature of the amorphous state leads to the likelihood of physical instability and recrystallisation promoted by external factors such as temperature or humidity.[3] Converting crystalline drugs to their amorphous counterpart is one of the most promising approaches in pharmaceutical material sciences in order to enhance APIs solubility and bioavailability. This strategy can be adopted only as long as a supersaturated solution of amorphous API can be maintained in the aqueous medium over time.[4]

Amorphous solid dispersions (ASDs) have been extensively used to stabilise supersaturated solution of APIs, resulting in a general increase of the oral bioavailability of poorly soluble drugs.[5–7] An ASD can be defined as a dispersion of one or more APIs in a solid-state inert carrier, usually an amorphous polymer,[8] and can be prepared by a range of manufacturing processes,[9] including spray drying[10], spray freeze drying[11], and hot melt extrusion[12]. Polymers such as polyethylene glycol (PEG),[13] and polyethylene oxide (PEO),[14] polyvinylpyrrolidone (PVP),[15] polyvinylpyrrolidone-polyvinyl acetate (PVP-VA),[16] hydroxypropylmethylcellulose (HMPC),[17] and hydroxypropylmethylcellulose acetyl succinate (HPMC-AS)[18] have been successfully used in ASDs. In particular, HPMC-AS has recently been suggested as a promising solid matrix to formulate ASDs[19] due to its high glass transition temperature, Tg, in the order of 120 °C,[20] its amphiphilic nature arising from the existence of hydrophilic (e.g., acetyl, A) and hydrophobic (e.g., succinoyl, S) functional groups, and the capability to tune the A and S contents.

It has been demonstrated that the polymer in ASDs plays a crucial role in stabilising the amorphous form of the drug.[21] The choice of a suitable polymer to formulate a specific dispersion largely depends on several chemical-physical properties such as Tg, thermal stability, dissolution profile, performance in dissolving API, and capability to stabilise amorphous drug.[22] These characteristics contribute to the stabilisation of the ASD which is due to the polymer's anti-plasticising effect, reducing molecular mobility of the amorphous API, and the formation of specific API - polymer interactions.[21] Intermolecular interactions such as hydrogen-bonding (H-bond), ionic forces, π-π, or electrostatic interactions are well established as the most significant interactions capable of stabilising such dispersed systems[4] by inhibiting recrystallisation phenomena in amorphous matrix and preventing competitive API - API or polymer - polymer intramolecular interactions. Recently HPMC-AS polymer[23] has been widely used to prepare ASD due its remarkable ability in stabilising amorphous dispersions arising from the formation of strong API - HPMC-AS interactions.[24]

The elucidation of the nature of the interaction between drugs and polymers and detecting recrystallised drugs in ASDs constitute some of the most significant challenges in pharmaceutical material sciences and require the exploitation of a range of characterisation approaches, often combining powder X-ray diffraction (PXRD), thermal analysis, vibrational methods and solid-state nuclear magnetic resonance (NMR) spectroscopy.[25,26] The PXRD patterns of amorphous solids result in broad diffuse scattering signals due to the lack of long-range order. Nevertheless, PXRD methods can provide significantly useful information on the residual crystalline content in ASDs, for example during stability studies.[27] Thermal analysis, including differential scanning calorimetry (DSC) and temperature-modulated DSC (mDSC),[28] have been employed to estimate the residual crystallinity in amorphous systems[29] and are often used to determine Tg values and detect thermal events revealing crystallisation and melting phenomena.[30] DSC therefore allows to detect miscibility of individual components of an ASD, where the observation of a single Tg indicates miscibility between API and polymer.[31] The Gordon-Taylor's (GT) model[32] can be used to estimate the Tg of an ideal binary mixture (Tg_{mix}) with significant deviations between predicted Tg_{mix} and experimentally determined Tg providing useful information about the interactions between the components in the mixture,[4,25,26] as the presence of API-API or API-polymer interactions can affect the Tg value of the system, while agreement suggests systems with absence of specific drug-polymer interactions. Furthermore, access to ASD stability can be also obtained using thermodynamic modelling and short to medium term physical stability of several API-polymer blend ASDs, including acetaminophen – HPMC-AS dispersions under controlled temperature and relative humidity (RH) conditions, have been determined for the 20 and 40% wt. formulation to be up to 6 and 1 month(s), respectively.[33] This work highlights a reduction of stability of these systems with the increase of the polymer content and an increase of RH.

A range of analytical methods including vibrational, Raman, Fourier-transform infrared spectroscopy (FT-IR) and solid-state nuclear magnetic resonance (NMR) spectroscopies have been used to provide atomic scale information about solid dispersions. Raman applications include the measurements of crystallisation rate[34] and mapping solid dispersions to identify and discriminate crystalline/amorphous domains.[35] FT-IR methods can be used to probe H-bonds for specific functional groups including hydroxyl, amino, and carbonyl groups when present in the API and/or the polymer molecular structure.[36] It has been demonstrated that when those functional groups are involving in H-bonding interactions, a simultaneous decrease in the stretching frequency and a widening of their absorption bands are observed due to smaller intermolecular distance between the donor-acceptor groups.[37]

NMR spectroscopy has proved itself as a powerful technique by providing an invaluable source of both structural and dynamics information at the atomic scale thereby being demonstrated as one of the most powerful method of characterisation. In particular, in the field of pharmaceutical sciences,[38,39] NMR allows the determination of the structure of drugs[40] and polymers.[41] Recently, NMR has emerged as a robust approach in (pharmaceutical) amorphous dispersions to identity site-specific API - polymer intermolecular interactions from changes in chemical shift values.[42–45] For example, using one dimensional (1D) and two dimensional (2D) NMR experiments, electrostatic interactions and H-bonding were identified in amorphous posaconazole (POSA) dispersion in HPMC-AS and involved the POSA's triazole and difluorophenyl ring moieties with some of the HPMC-AS's substituent groups.[44] The presence of π-π aromatic packing interaction between POSA and HPMC-phthalate (HPMC-P) amorphous dispersion have also been highlighted.[44] Drug-polymer interactions in carbamazepine (CBZ) in HPMC, HPMC-A, and HPMC-S dispersions have also been established[42] and identified H-bonding between the CBZ's -NH_2 group with the acetyl moiety in HPMC-A, and between both CBZ -NH_2's and carbonyl groups of the succinyl group in HPMC-S. This demonstrates the important role that both acetyl and succinyl groups of HPMC-AS could play in the formation of stable API-polymer connections. 2D NMR techniques that include homonuclear and heteronuclear correlation spectroscopy are widely used to detect intramolecular interaction by exploiting the homo- and heteronuclear through space dipolar coupling between the nuclei. In order to increase the NMR sensitivity and hence to have access to high-resolution spectra and enabling proton detection, the use of ultrafast Magic Angle Spinning (MAS) experiments, with frequency in the 50 - 110 kHz range, have also recently emerged. They enable fast characterisation of pharmaceutical compounds and how they formulate by probing API-polymer interaction,[45] allowing NMR crystallography approaches[46] and understanding of low drug loaded formulation.[47] The ^{14}N-^{1}H heteronuclear multiple-quantum coherence (HMQC)[48] experiment carried out at high magnetic field and at ultrafast MAS conditions under direct ^{1}H signal detection has been robustly employed to probe interactions in crystalline systems[49,50] and recently to highlight molecular association and interactions in amorphous dispersions.[51,52] ^{14}N-^{1}H HMQC spectra were used to identify hydrogen bonding interaction in a nicotinamide palmitic acid cocrystal and acetaminophen - PVP amorphous dispersion.[50] The versatility of this experiment was demonstrated by providing information on the symmetry of the nitrogen environment and through-space proximities in paclitaxel loaded polymer micelles amorphous formulations.[52] The ^{14}N-^{1}H HMQC experiment has however, to the best of our knowledge, not been used so far to investigate API-polymer interactions in HPMC-AS based amorphous formulations.

Here, we report the stability of amorphous acetaminophen in HPMC-AS ASDs at different drug loadings by identifying the presence of drug-polymer intramolecular interactions with multinuclear multidimensional NMR experiments. Acetaminophen (Figure 1, and supporting information Figure SI-1) is one of the most widely used API and its chemical-physical data, including melting point and solubility profiles, as well as crystalline data,[53,54] NMR spectra,[55] are largely known. HPMC-AS polymer was chosen as excipient due to its excellent capacity to stabilise amorphous dispersion.[42,44]. Morevoer, the lack of overlap between acetaminophen and polymer signals in the ^{13}C NMR spectra allows monitoring of the changes in chemical shift and line width of the signals of both components in order to establish API-polymer interactions and crystalline/amorphous behavior. Multidimensional multinuclear MAS NMR data enable access to structural information in the solid state, highlighting the presence of API - polymer intermolecular interactions for ASDs with drug loading < 20% wt. and providing useful indications of their stability. The approach also suggests the absence of API - polymer intermolecular interaction in the 40% wt. ASD and rather identifies signals corresponding to crystalline acetaminophen interacting with itself.

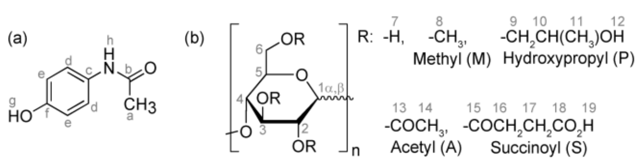

Figure 1. Chemical structure of (a) acetaminophen and (b) HPMC-AS polymer. HPMC-AS consists of a cellulose ring bonded with various R groups that include hydrogen, methyl (M), hydroxypropyl (P), acetyl (A), and succinoyl (S) groups. The wavy bond in the cellulose ring indicates that cellulose ring can exist in two different cyclic hemiacetal configurations, called α- and β- glucopyranose, distinguishable from the different configurations of the anomeric carbon C_1. The lettering and numbering are used for all NMR spectral assignments throughout.

2 Experimental section

2.1 Materials

ASDs were prepared using acetaminophen form I (99.5 %) purchased from Spectrum Chemical Company and HPMC-AS polymer M grade obtained from Shin-Etsu Chemical Co. (lot # 6033060, M content = 23.4 %, P content = 7.3%, A content = 8.8%, and S content = 11.2%). Sigma-Aldrich's acetaminophen form I was used to carried out the PXRD analysis. The dipeptide β-AspAla was obtained from Bachem. All materials were used as received.

2.2 Synthesis of ASDs

General procedure of the preparation of ASDs: Gram-scale batches formulated at 10, 20 and 40%, wt. of acetaminophen were manufactured using a custom-built small-scale spray dryer. Spray dry solution of acetaminophen and polymer containing 2.5% solid (acetaminophen and HPMC-AS) were sprayed at 65-70 °C from acetone (80 mL) using heated nitrogen gas through a two-fluid spraying nozzle (2050 LC/64AC, Spraying Systems Co). The ASD was then collected by filtration from the spray dryer and dried overnight *in vacuo*. ASDs were stored in a freezer kept at low temperature (-80 °C) to prevent API recrystallisation.

Synthesis of 10% wt. acetaminophen in HPMC-AS ASD: This formulation was prepared according to the general procedure highlighted above using acetaminophen (0.2 g, 1.3 mmol) and HPMC-AS (1.7 g).

Synthesis of 20% wt. acetaminophen in HPMC-AS ASD: This formulation was prepared according to the general procedure highlighted above using acetaminophen (0.4 g, 2.7 mmol) and HPMC-AS (1.6 g).

Synthesis of 40% wt. acetaminophen in HPMC-AS ASD: This formulation was prepared according to the general procedure highlighted above using acetaminophen (0.8 g. 5.3 mmol) and HPMC-AS (1.2 g).

2.3 PXRD measurements

Laboratory PXRD data were collected using a PANalytical Empyrean diffractometer equipped with a high throughput Transmission geometry, focusing mirror, 1/2 degree divergence, and anti-scatter slits, 4 mm beam mask, 0.04-degree soller slits, with Cu-Kα of 1.541874 Å. PXRD patterns were measured over the 2θ range 2−40° over 1 hour.

2.4 Standard and modulated DSC measurements

DSC experiments were performed using a DSC Q1000 (TA Instruments, DE, USA) system using TA-Tzero aluminium pans loaded with an amount of around 10 mg of sample. Standard DSC analyses were carried out using a cool-heat-cool cycle method in which the sample was cooled to -15 °C and heated up to 160 °C with a ramp of 10 °C/min, and then after an isotherm of 5 min, a cool ramp of 20 °C/min was applied back down to -15 °C. mDSC experiments were carried out using a heating ramp of 2.5 °C/min with a modulation amplitude of 1.5 °C every 60 s.

2.5 Solid State NMR experiments

^{1}H NMR spectra were recorded on a Bruker 800 MHz (18.8 T) Avance Neo NMR spectrometer using a Bruker 1.3 mm HX MAS probe or on a Bruker 850 MHz (20 T) Avance Neo spectrometer equipped with 1.3 mm triple-resonance HXY MAS probe in double resonance (DR) mode. All the spectra were recorded under a MAS frequency of ν_r = 60 kHz. ^{1}H pulses were carried out at a radio frequency (rf) field magnitude of 100 kHz. ASDs ^{1}H spin-lattice relaxation times T_1 were recorded at 18.8 T from saturation recovery experiments and fitted to a stretch exponential function 1-exp[-($\tau/T_1)^{\alpha}$] in which τ is the variable delay and α the stretch factor ranging from 0.5 and 1.

All $^{13}C/^{15}N$ cross polarisation (CP) and two-dimensional 2D ^{1}H-$^{13}C/^{15}N$ CP heteronuclear correlation (HECTOR) experiments were performed on a Bruker 400 MHz (9.4 T) Avance III HD NMR spectrometer equipped with a 4 mm triple-resonance HXY MAS probe in DR mode tuned to ^{1}H and ^{13}C or ^{15}N at Larmor frequencies of 400.1, 100.6 and 40.5 MHz, respectively. ^{1}H pulses and SPINAL-64 heteronuclear decoupling[56] during $^{13}C/^{15}N$ detection were carried out with rf field amplitude of 83 kHz. All experiments were performed under a MAS frequency of ν_r = 12.5 kHz for ^{13}C and 10 kHz for ^{15}N and using a recycle delay of 1.3 x ^{1}H T_1s obtained as above (data at 9.4 T not given). The Hartmann-Hahn[57] conditions for ^{13}C CP were achieved using a ^{13}C rf amplitude of around 45 kHz ramped to obtain maximum signal at a ^{1}H rf field of 60 kHz, and for ^{15}N CP, a ^{15}N rf amplitude of 28 kHz ramped to obtain maximum signal at a ^{1}H rf field of 50 kHz was used. A 2 ms contact time during ^{13}C CP and optimised CP contact times of 1 ms for amorphous material and 6 ms for crystalline sample during ^{15}N CP were used. ASDs ^{1}H spin-lattice relaxation times in the rotating frame ($T_{1\rho}$) were obtained at 9.4 T, using a spin-lock pulse sequence through ^{13}C detection via CP, at ^{1}H frequencies of $\omega_1/2\pi$ of 40 and 83 kHz and fitted to a stretch exponential function of the form exp[-($\tau/T_{1\rho})^{\beta}$] (with β ranging between 0.2 to 1). ^{13}C T_1s were obtained at 9.4 T from ^{13}C inversion recovery via CP experiments and fitted to an expression of the form exp[-($\tau/T_1)^{\gamma}$] (with γ ranging from 0.4 to 1). Frequency switched Lee-Goldberg (FSLG) homonuclear decoupling[58] during the ^{1}H t_1 evolution time in the 2D CP HETCOR spectra was obtained at a rf amplitude of 83 kHz and an offset of 60 kHz. Experimentally determined ^{1}H scaling factors λ_{exp} for FSLG (as measured on L-alanine using the experimental conditions given above) were used to recover the full ^{1}H chemical shifts $\delta(^{1}H)^{MAS}$ from the scaled down apparent chemical shifts $\delta(^{1}H)^{APP}$ according to $\delta(^{1}H)^{APP} = \lambda_{exp}\delta(^{1}H)^{MAS}$ that result from this decoupling.

^{14}N-^{1}H HMQC experiments were carried out using a Bruker 800 MHz (18.8 T) Avance Neo NMR spectrometer equipped with a Bruker 1.3 mm HX MAS probe tuned to ^{1}H and ^{14}N at 800.3 and 58.7 MHz, respectively, or using a Bruker 850 MHz (20.0 T) Avance Neo NMR spectrometer equipped with a 1.3 mm triple resonance HXY MAS probe operating in DR mode tuned to ^{1}H and ^{14}N at 850.2 and 61.4 MHz, respectively. Experiments were performed under a MAS frequency ν_r = 60 kHz. In the ^{14}N-^{1}H HMQC pulse sequence used, heteronuclear dipolar couplings were reintroduced via rotary resonance recoupling, R^3,[59] on the n = 2 resonance condition,[48] using an x, -x phase inversion[60] of individual block lengths of one rotor period of 16.7 µs at rf amplitude of 120 kHz (2 x MAS frequency). ^{1}H and ^{14}N pulses were performed at rf amplitude of 100 and 72 kHz, respectively. HMQC spectra were processed after removal of the first few points in the free-induction-decay (FID) using a home-built macro running on TopSpin to reduce baseline distortion and residual t_1 noise from the spectrum.

^{1}H, ^{13}C and ^{15}N spectra were externally referenced to the NH proton of the dipeptide β-AspAla at 8.0 ppm,[50] the tertiary carbon of adamantane at 29.45 ppm,[61] and to glycine at -347.2 ppm,[62] respectively. ^{14}N shifts were referenced to solid NH_4Cl at -341.3 ppm[62] which has a cubic ^{14}N site.[63] Magic angle calibrations were achieved by maximising either the separation of NH_3 and NH resonances of the dipeptide β-AspAla in the ^{14}N-^{1}H HMQC spectrum or the number of rotational resonances in the time domain of the ^{79}Br spectrum of KBr. The errors associated with ^{1}H, ^{13}C, ^{15}N chemical shifts and ^{14}N parameters are given in the respective tables. ^{1}H $T_{1\rho}$ and ^{13}C T_1 fitting data were carried out using MATLAB R2017a. Deconvolution of the experimental spectra was carried out in TopSpin 4.0.5 using the solid line shape analysis routine.

3 Results and discussion

3.1 PXRD characterization

Acetaminophen exists in three polymorphic forms:[53,64,65] monoclinic form I (space group $P2_1/a$, and number of asymmetric unit in the cell, Z' = 1) which is the most thermodynamically stable form; orthorhombic form II (space group P*cab*, Z' = 1) polymorph, and a highly metastable form III (space group $Pca2_1$, Z' = 2). Time-dependent PXRD patterns measurements (Figure 2) on acetaminophen – HPMC-AS ASDs at 10% wt. (in dark blue), 20% wt. (in orange) and 40% wt. (in

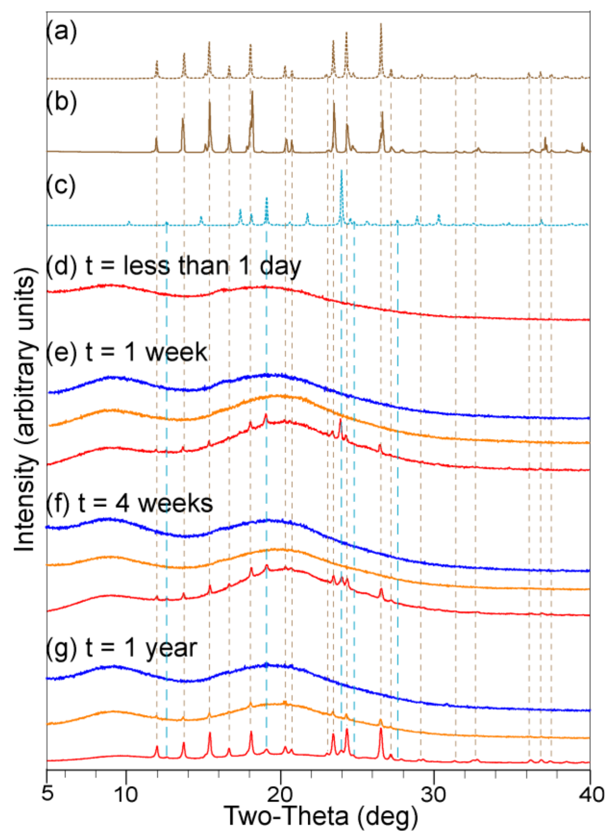

Figure 2. PXRD patterns of (a) simulated acetaminophen form I from CSD (refcode HXACAN01, brown dotted lines)[64], (b) experimental acetaminophen form I (brown full lines), and (c) simulated acetaminophen form II from CSD (refcode HXACAN23, light blue dotted lines)[64]. Comparison of XRD patterns of 10% wt. (dark blue), 20% wt. (orange) and 40% wt. (red) for the acetaminophen – HPMC-AS ASDs at times of (d) less than 1 day, (e) 1 week, (f) 4 weeks, and (g) 1 year at RT (around 20 °C) and ambient RH (ranging from 30 to 50%). After 1 year, the 10% wt. ASD still shows an amorphous state while, in the 20% wt. traces of recrystallisation to acetaminophen l is observed and further confirmed by the ^{13}C CP HETCOR spectra (Figure SI-2). In 40% wt. ASD, acetaminophen forms I and II are detected after only 1 week.

red) loadings were carried out over a one-year period of exposure at room temperature (RT, around 20 °C) and ambient relative humidity (RH, ranging from 30 to 50%) to monitor the chemical stability of the systems and potential recrystallisation phenomena. The diffraction patterns of the 10% wt. (in dark blue) ASD exhibit the typical broad signal of an amorphous material and the absence of Bragg peaks up to 1 year, indicating a strong tendency of this system to remain in the amorphous state. The 20% wt. ASD shows a typical broad signal of an amorphous material only up to 4 weeks at RT and ambient RH after which reflections from acetaminophen form I start to appear. This is in sharp contrast with the PXRD data in 40% wt. ASD that shows recrystallisation after only 1 week and, interestingly, to a mixture of both acetaminophen form I and II polymorphs

3.2 Thermal characterization

The GT model was used to estimate the predicted Tg_{mix} values of the acetaminophen – HPMC-AS dispersion at different drug loading wt. % from the following expression:

$$Tg_{mix} = \frac{w_{acetaminophen} Tg_{acetaminophen} + k w_{HPMC\text{-}AS} Tg_{HPMC\text{-}AS}}{w_{acetaminophen} + k w_{HPMC\text{-}AS}} \quad (1)$$

where w and Tg are the weight fractions and glass transition temperature of each components, respectively, and k a constant related to the density ρ ($\rho_{acetaminophen}$ = 1.29 gcm^{-3}, $\rho_{HPMC\text{-}AS}$ = 1.28 gcm^{-3})[33] and given by:

$$k \approx \frac{\rho_{acetaminophen} Tg_{acetaminophen}}{\rho_{HPMC\text{-}AS} Tg_{HPMC\text{-}AS}} = 0.8 \quad (2)$$

Supporting information Table SI-1 summarises Tgs for the individual components as well as the predicted and experimental Tg_{mix} values obtained for the 10% wt., 20% wt., and 40% wt. ASDs with negative deviations from predicted Tgs represented in Figure 3. This demonstrates non ideal drug-polymer mixture,[7] the negative deviations suggesting that intramolecular interactions between like species (drug-drug or polymer-polymer) dominate, however, importantly, not excluding the presence, to a lesser extent, of intramolecular drug-polymer interactions (see below).[66] Additionally, negative deviations can also be interpreted as being indicative of non-ideal additivity of volume for the two components and points out of a likelihood of phase separation of the system.[67] The largest deviation is found for the 40% wt. solid dispersion and suggests that at, amongst the ASDs studied, recrystallisation phenomena and phase separation occur more quickly in this formulation.

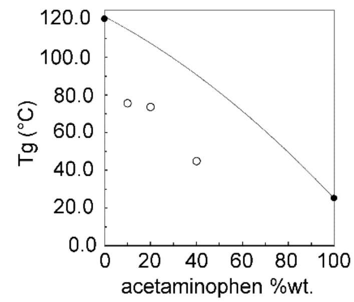

Figure 3. Tg values of acetaminophen – HPMC-AS dispersions obtained at different acetaminophen loading in HPMC-AS polymer based ASDs. Experimentally obtained values for the ASDs, individual components and predicted values from the GT model based on equation 1 are given in empty circles (○), filled circles (•) and solid line, respectively.

3.3 Solid-State NMR data

Figure 4(a) compares the ^{13}C CP MAS spectra of acetaminophen form I, HPMC-AS polymer, 10% wt., 20% wt., and, 40% wt. ASDs. The spectrum of acetaminophen form I presents resonances at around 170 ppm for the carbonyl (C_b^I), 152-116 ppm for the aromatic carbons (C_f^I, C_c^I, C_d^I, C_e^I) and 24 ppm for the methyl carbon (C_a^I) (see Figure 1(a) and Table SI-2) ('I' indicates characteristic resonances for the acetaminophen form I) based on previous literature.[68] The four peaks in the region 105 - 60 ppm in the spectrum of HPMC-AS polymer (Figure 1(b)) can be attributed to the anomeric C_1, C_4, $C_{2,3}$, and $C_{5,10}$ carbons while the shoulders at around 70 and 58 ppm correspond to $C_{6,9}$ (CH_2s) and C_8 (methoxy group), and the three peaks in the aliphatic region to $C_{16,17}$ (CH_2 of the S group), C_{14} (CH_3 of the A group), and C_{11} (methyl group of the P moiety),

Table 1. Selected significant changes in ^{13}C chemical shifts. A comprehensive list of ^{13}C chemical shifts is given in Table SI-2.[a]

Signal	Acetaminophen form I	HPMC-AS	10% wt. ASD	20% wt. ASD	40% wt. ASD	Recrystallised 40% wt. ASD
$C_{15,18}$	n.a.	174	174	177	176	174.9
C_{13}	n.a.	171	172	173	173	172.4
C_b	169.7	n.a.	171	171	171	169.8$^{(I/II)}$
C_f	152.2	n.a.	154	154	154	153.8$^{(II)}$, 152.2$^{(I)}$
C_c	132.9	n.a.	131	131	131	132.9$^{(I)}$, 130.76$^{(II)}$
C_d	123.3, 120.5	n.a.	121	121	121	123.3$^{(I)}$, 120.5$^{(I/II)}$
C_e	116.3, 115.6	n.a.	116	116	116	118.3$^{(II)}$, 115.7$^{(I)}$

[a] Values are given in ppm. The ^{13}C chemical shifts of all assigned resonances are quoted within an accuracy of ± 1 ppm due to the broad line widths associated with amorphous samples, except for the crystalline species where they are quoted at ± 0.5 ppm. 'I' and 'II' indicate resonances belonging to acetaminophen form I and II, respectively.

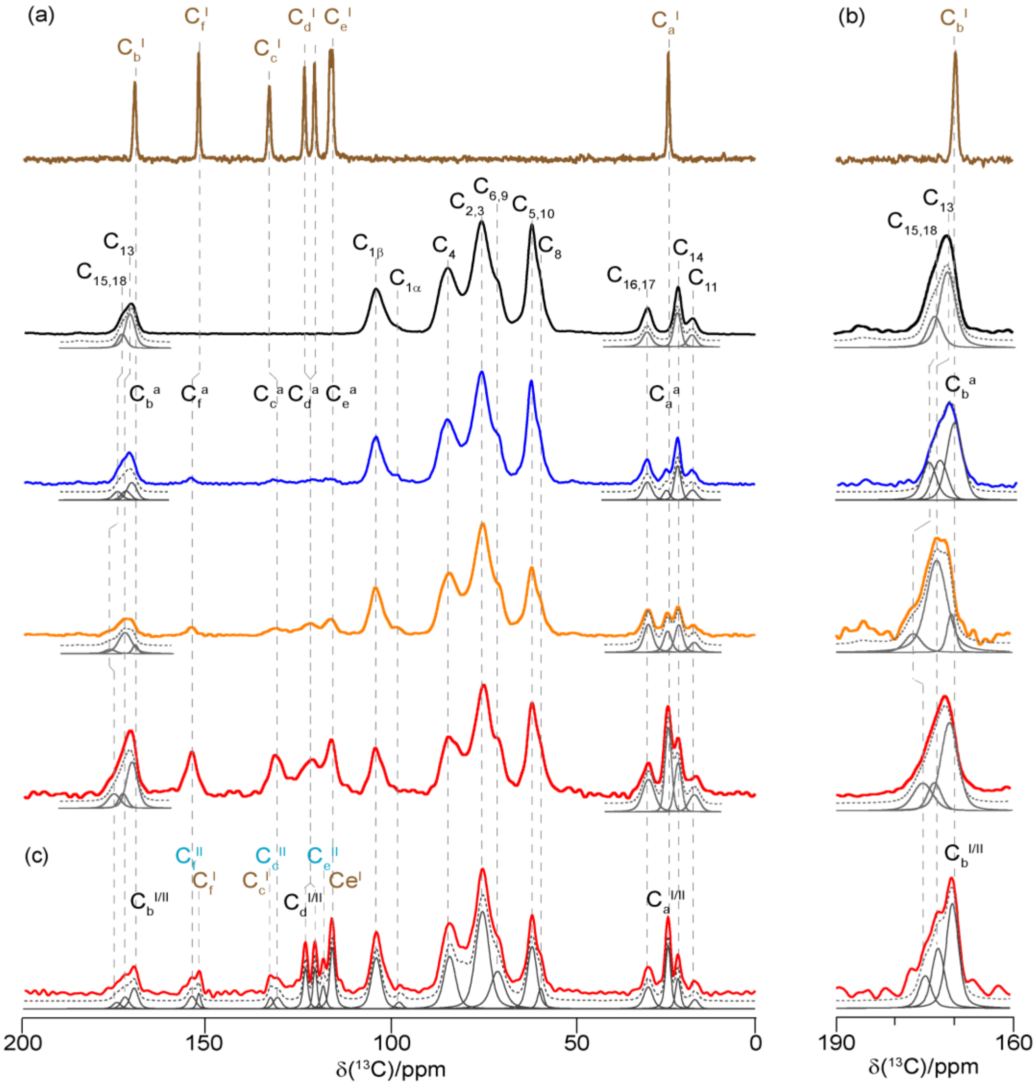

Figure 4. (a) ^{13}C CP MAS spectra of crystalline acetaminophen form I (brown), HPMC-AS (black),[69] 10% wt. (dark blue), 20% wt. (orange), and 40% wt. acetaminophen – HPMC-AS ASDs (red) recorded at less than 1 day at RT/ambient RH. (b) Magnified view of the 190-160 ppm (carbonyl region) of all the spectra. (c) ^{13}C CP spectrum of the 40% wt. dispersion towards recrystallisation after 1 week at RT/ambient RH. A magnified view of this spectrum is given in the aromatic region is given in Figure SI-3. For spectral identification, simulated spectra (dashed grey lines) and spectral deconvolution (grey lines) are also shown. The notations 'I' and 'II' indicate the characteristic resonances for the acetaminophen forms I and II, respectively while the notation 'a' indicates resonance that can be attributed to amorphous acetaminophen.

respectively. Deconvolution in the carbonyl region of the HPMC-AS polymer reveals two signals assigned to $C_{15,18}$ (most shifted peak, S substituent the *C*Os) and C_{13} (A's *C*O).[69] The knowledge of the ^{13}C assignment of both drug and HPMC-AS polymer plays an important role in the identification of drug-polymer interactions in ASDs as this is largely based on change in chemical shifts.[4,43] The ^{13}C assignments for the ^{13}C CP MAS NMR spectra of all ASDs, recorded at less than 1 day at RT/ambient RH, are based on the known spectra of HPMC-AS[69] and acetaminophen form I[68] (Table SI-2). In the spectra of the ASDs, signals assignable to the amorphous acetaminophen generally appear broader than in the crystalline form as expected from amorphisation as the loss of crystallinity brings of a range of chemical environments present that are randomly distributed in the sample resulting in severe inhomogeneous line broadening.[43] The decreased resolution is evident from of the absence of split signals of the aromatic carbons of acetaminophen (C_d^I and C_e^I), due to the lack of crystal packing, indicating the presence of amorphous acetaminophen. This is further confirmed by a significant shortening of ^{13}C T_1 values by up to two orders of magnitude from acetaminophen form I to the amorphous acetaminophen in the ASD (Table SI-3). Meanwhile, the ^{13}C T_1 values for HPMC-AS in the ASDs are slightly increased, presumably indicating an increase in rigidity when formulated and suggesting its co-binding in API-polymer interactions (see below). In addition, ^{13}C NMR signals for C_d^I/C_e^I and quaternary carbons C_f^a show a small difference in chemical shifts of 2-3 ppm *vs.* acetaminophen form I (Table 1). This

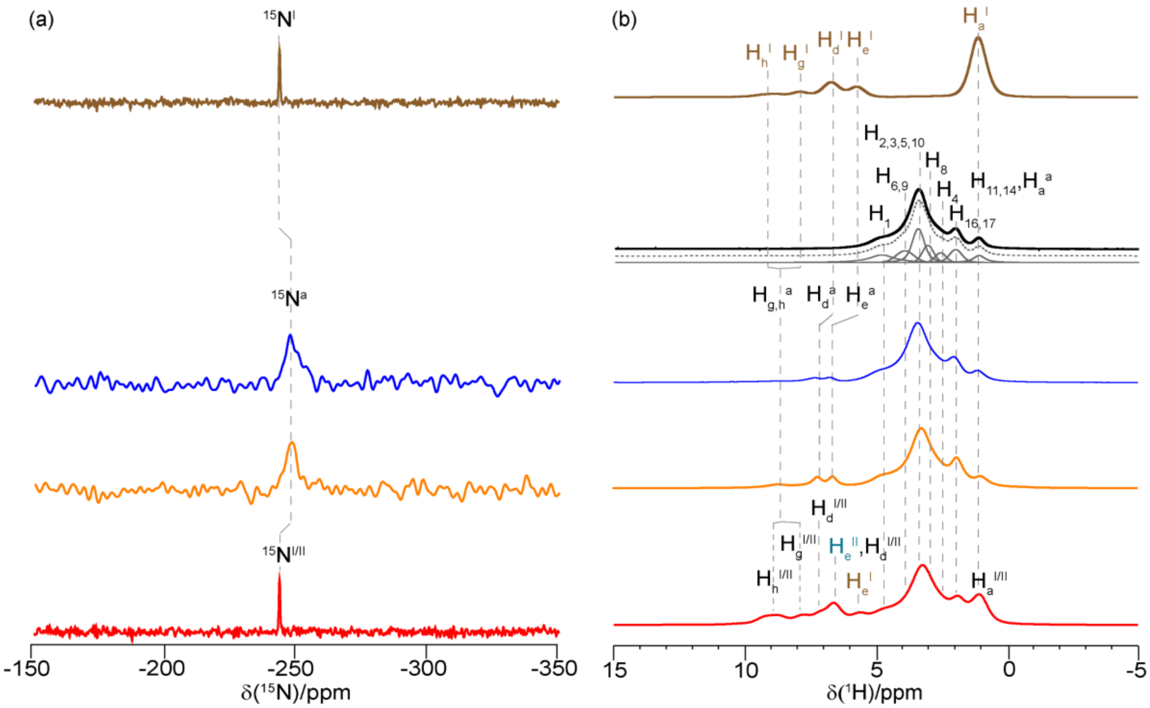

Figure 5. (a) ^{15}N CP MAS spectra of crystalline acetaminophen form I (brown), 10% wt. (dark blue) 20% wt. (orange), and 40% wt. (red) acetaminophen – HPMC-AS ASDs. (b) Quantitative ^{1}H spectra of crystalline acetaminophen form I (brown), HPMC-AS (black), 10% wt. (dark blue), 20% wt. (orange), and 40% wt. (red) acetaminophen HPMC-AS ASDs after recrystallisation. ^{1}H signals assignment is based on the ^{13}C and ^{15}N CP HETCOR experiments in Figure 6(a) and Figure SI-5, respectively. Magnified views of both ^{15}N CP and ^{1}H spectra can be found in Figure SI-6 and SI-7, respectively.

suggests structural change in the amorphous systems[43,45,70] attributed to crystalline API conversion to its amorphous form[71] and results from the absence of long-range 3D interactions (e.g., hydrogen-bonding, π-π interactions) in the crystalline sample, resulting in variation of local electronic environments.

Furthermore, and more importantly, the carbonyl carbons of the A and S units ($C_{15,18}$ and C_{13}) in the ASDs appear to be sensitive to the amount of amorphous acetaminophen in the ASDs as a slight change in chemical shifts *vs.* HPMC-AS to higher frequency is observed (Figure 4(b) and Table 1), as shown by the deconvoluted signals for the 190–160 ppm region of the spectra that assumed the presence of three carbonyl signals C_b, $C_{13,15}$ and C_{18}, "three signals model" and supported by residual spectra (Figure SI-4). These shifts are ascribed to API - polymer intramolecular interaction in ASDs and detect molecular association via H-bonding in dispersions,[31,72,73] as previously observed in the Posaconazole (POSA) and HPMC-AS ASD.[44]

The ^{13}C CP MAS NMR spectrum of the 40% wt. ASD was also recorded after 1 week under ambient condition (Figure 4(c)) and shows significant differences with the one obtained at less than 1 day at RT/ambient RH. The spectrum exhibits a number of additional and sharper peaks as well as a lengthening of the ^{1}H T_1's (Table SI-4) indicating the presence of crystalline acetaminophen arising from fast recrystallisation from the ASDs. The resonances observed in Figure 4(c) (a magnified view of this spectrum is given in the aromatic region is given in Figure SI-3) indicates the presence of signals that can be attributed to both acetaminophen form I (Figure 4(a), brown) and II[68] as anticipated from the PXRD data (Figure 2). The

Table 2. Experimental ^{15}N isotropic chemical shifts $\delta_{iso}(^{15}N)$, ^{14}N shifts $\delta_{iso}(^{14}N)$, ^{14}N quadrupolar-induced shifts δ^{Q}_{iso} and quadrupolar products P_Q.

Sample	$\delta_{iso}(^{15}N)^a$	$\delta_{iso}(^{14}N)^a$	$\delta^{Q}_{iso}(^{14}N)^a$	$P_Q{}^b$
Acetaminophen form I[51,c]	-244	-125	119	2.5
10% wt. ASD [c]	-247	-75	172	2.9
20% wt. ASD [d]	-247	-80	167	2.9
Recrystallised 40% wt. ASD [c]	-243	-67	176	2.9

[a] Shifts are given in ppm. $\delta_{iso}(^{15}N)$ values are obtained from the peak positions in the ^{15}N CP MAS spectra (with an associated error of ± 1 ppm) while $\delta_{iso}(^{14}N)$ values represent the centre of gravity of the ^{14}N line shape extracted from the ^{14}N-^{1}H HMQC spectra (with an associated error of ± 5 ppm). Magnetic field dependent ^{14}N shifts quoted in the table are given for 20 T. [b] P_Q values are given in MHz, with an estimated error of ± 0.1 MHz, and obtained from Eq. 5. [c] Experimental data obtained at 20 T. [d] Experimental data obtained at 18.8 T (Table SI-5) and quoted at 20 T.

presence of signals attributable to the two polymorphs of acetaminophen in 40% wt. ASD strongly indicates the instability of this dispersion towards recrystallisation and could be reasonably explained by the lack of any interaction between acetaminophen and HPMC-AS, as predicted by the significant negative deviation from the GT model (Figure 1). Figure 5(a) compares the ^{15}N CP MAS NMR spectra of acetaminophen form I, 10% wt. and 20% wt. amorphous acetaminophen in HPMC-AS solid dispersion which show one signal assignable to the acetaminophen NH amide group (Figure 1(a)). This peak resonates at -243 ppm and is fairly narrow (full-width-at-half maximum, FWHM of 26 Hz) which is consistent with the literature data for acetaminophen form I[68], while the signal appears at -247 ppm for both 10% wt. and 20% wt. ASDs and is significantly broader (FWHM of 240-260 Hz). The change in the ^{15}N chemical shift and broadening of the ^{15}N spectra observed between crystalline and amorphous species suggests a different hydrogen-bonding network and intramolecular interactions (Table 2).[42,45,74] The ^{15}N CP spectrum of the 40% wt. ASD shows a single resonance at -243 ppm (FWHM of 24 Hz) at the same chemical shift for crystalline form I and likely arises from acetaminophen that underwent recrystallisation during data acquisition. Although acetaminophen forms I and II in the 40% wt. ASD have been observed in both PXRD and ^{13}C NMR data, the two expected ^{15}N signals are not resolved at 9.4 T, likely due to their very similar chemical shift values only separated by 0.4 ppm.[68]

The ^{1}H MAS NMR spectrum (Figure 5(b)) of acetaminophen form I, obtained under high magnetic field (> 18.8 T) and very fast MAS frequency (> 50 kHz), shows fairly resolved resonances at around 9.0, 7.9, 6.7, 5.7 and 1.1 ppm assigned to -NH and -OH groups, aromatic protons (H_d^I and H_e^I) and methyl groups, respectively. In the HPMC-AS spectrum, the three main peaks, and the peak at 1.1 ppm can be assigned to H_1, $H_{2,3,5,10}$, $H_{16,17}$, and $H_{11,14}$, respectively, while spectral deconvolution reveals additional signals at 3.9, 3.0, and 2.5 ppm that are assigned to $H_{6,9}$, H_8, and H_4, respectively. Due to possible exchange phenomena, the H_7, -O*H* (hydroxypropyl substituent group) and the -CO_2*H* (succinoyl moiety) proton signals (Figure 1) are not observed in the 1D and ^{13}C CP HETCOR spectra.

The ^{1}H spectra of HPMC-AS and all three ASDs (Figure 5(b)) are assigned from correlations observed in the ^{13}C CP HETCOR spectra recorded at a short contact time (Figures 6(a)), ^{15}N CP HETCOR spectrum of the 20%wt (Figure SI-5) and known ^{1}H chemical shifts. The ^{1}H spectra of the ASDs (Figure 5(b)) show a cluster of signals around 5 and 1 ppm, corresponding HPMC-AS, as well as additional resonances for the acetaminophen. As summarised in Table 3, in the 10% wt. and 20% wt. ASDs, the aromatic proton signals (H_d^a and H_e^a) are deshielded with respect the crystalline counterpart, the small difference observed being typical of amorphisation processes.[71] Finally, the H_g^a and H_h^a signals merged into a single broad signal centred at 8.5 ppm which correlates strongly with the ^{15}N signal as revealed by the ^{15}N CP HETCOR spectrum (Figure SI-5), potentially confirming the absence of deprotonation. It has been demonstrated that deprotonation effect, promoted by the solvent during the spray dry process, might impact API-polymer interactions.[45] It is well known that evaluation of the length scale of spin diffusion allows the degree of mixture miscibility to be determined by recording the ^{1}H relaxation times of all components.[75–78] ^{1}H T_1 and $T_{1\rho}$ values have

Table 3. Significant changes observed in ^{1}H chemical shifts for selected protons.[a]

Signal	Acetaminophen form I	10%wt. ASD	20%wt. ASD	Recrystallised 40% wt. ASD
H_h	9.0	8.5	8.5	9.0 (I/II)
H_g	7.9	8.5	8.5	7.9 (I/II)
H_d	6.7	7.4	7.4	7.2 (I/II), 5.7 (I/II)
H_e	5.7	6.8	6.8	6.8 (II), 5.7 (I)

[a] Values are given in ppm. A comprehensive list of ^{1}H chemical shifts can be found in Table SI-7. The associated error with the chemical shift values is ± 0.2 ppm.

therefore been measured for the API and polymer in the ASD (Tables SI-4 and SI-6) and revealed that, for the 20% wt. formulation, they are similar (e.g., ^{1}H T_1 values for H_d^a and H_1 are 1.7 ± 0.2 s and 1.9 ± 0.3 s, respectively, and ^{1}H $T_{1\rho}$ (H_d^a) = 3.8 ± 1.1 ms ≈ ^{1}H $T_{1\rho}$ (H_1) = 4.4 ± 0.3 ms at a spin lock frequency of 40 kHz), indicating, that in the 2-5 nm length scale,[79] there is miscibility in the acetaminophen – HPMC-AS ASD. In contrast, significantly different ^{1}H T_1 and $T_{1\rho}$ values are obtained for the recrystallised 40% wt. dispersion (Table SI-6) suggesting that phase separation phenomena occur in a domain size larger that 20 – 50 nm.[79]

Through space ^{13}C CP HETCOR experiments recorded at a longer contact time (in the range of ms) allows observation of acetaminophen-polymer interactions with correlation signals providing direct evidence of intermolecular drug polymer interactions. The corresponding ^{13}C CP HETCOR spectra of both 10% wt. and 20% wt. ASD identified correlation signals between peaks in ^{13}C at 120-150 ppm corresponding to acetaminophen with ^{1}H at 3 ppm (shaded signals in Figure 6(b)). These spatial correlations, detected via the strong ^{13}C-^{1}H heteronuclear dipolar coupling due to the rigid protons on the cellulose ring, cannot be ascribed to intramolecular correlations within acetaminophen due to the absence of ^{1}H signals at this shift (Figure 5(b)), but rather intermolecular acetaminophen – HPMC-AS interaction involving the aromatic carbons of acetaminophen with the backbone cellulose ring's protons of the polymer.

In sharp contrast, the ^{13}C CP HETCOR spectrum of 40% wt. ASD identifies correlated signals corresponding to crystalline acetaminophen interacting with itself as shown by the shaded signals in Figure 6(b) (no 2D correlation is observed for the broader shoulders of the 1D spectrum likely due to poor signal-to-noise ratio in the HETCOR of the minor amorphous acetaminophen species). This suggests the absence of acetaminophen – HPMC-AS intramolecular interaction and indicates a two-phase immiscible system in which API-API interactions dominate, in good agreement with GT predictions, the presence of acetaminophen recrystallisation and validating ^{1}H relaxation data (see above), thereby confirm the instability of this ASD at the atomic level.

^{14}N-^{1}H HMQC experiments were then deployed under optima conditions of high magnetic field and very fast MAS frequency to establish the involvement of the amide nitrogen in the intermolecular interactions in these ASDs. ^{14}N is a high abundance spin (99.6 %) but due to its low gyromagnetic ratio (1.93 ×10^7 rad T^{-1} s^{-1}) and spin quantum number I = 1, ^{14}N has low sensitivity and exhibits quadrupole interaction, leading to a significant signal broadening. For these reasons, the direct

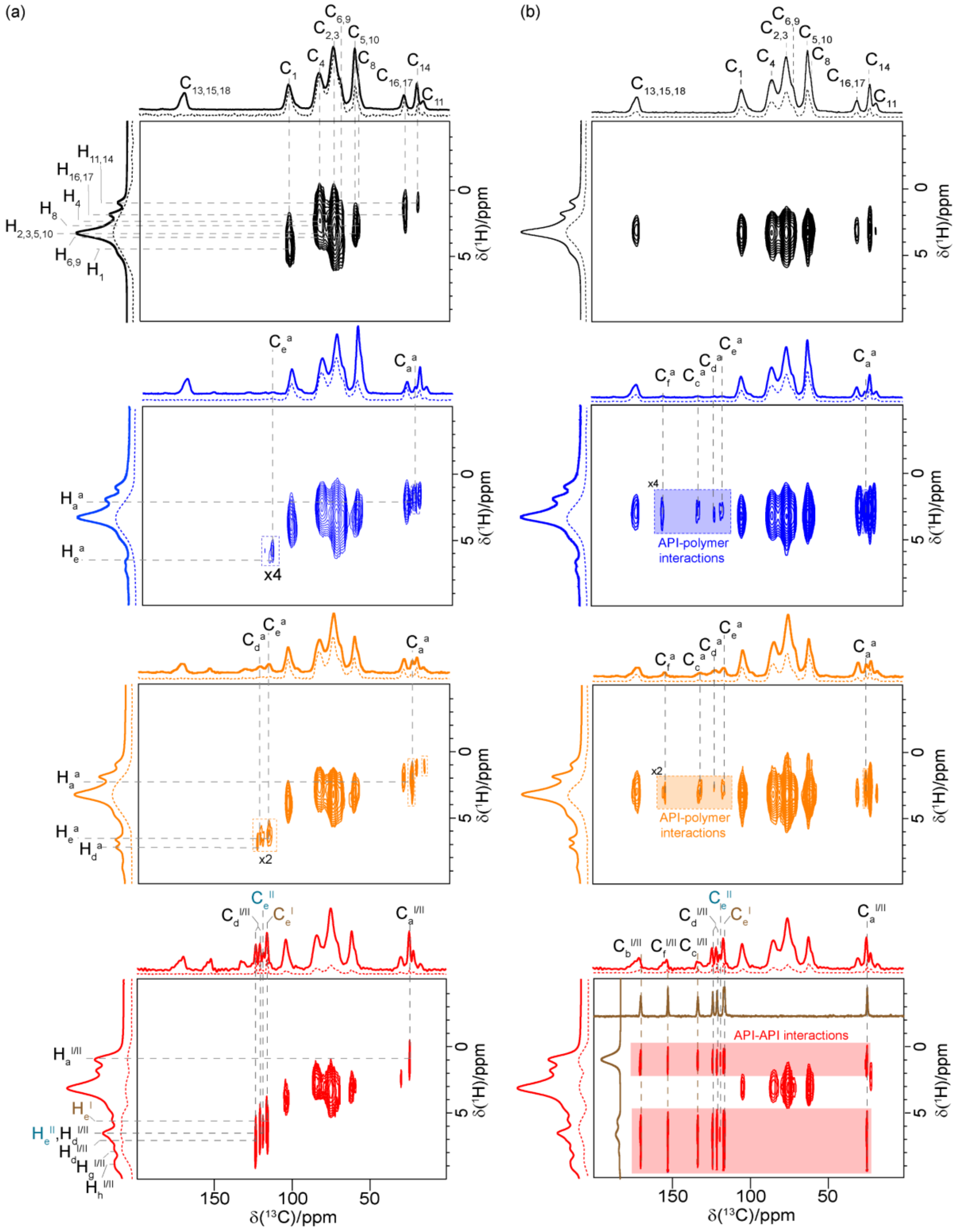

Figure 6. ^{13}C CP HETCOR spectra of HPMC-AS (black), 10% wt. (dark blue), 20% wt. (orange) and 40% wt. (red) acetaminophen HPMC-AS ASD recorded with a contact time of (a) 50 µs and (b) 2 ms. Correlations were used for ^{1}H spectral assignments. Top: ^{13}C CP MAS spectra at a contact time of 2 ms. Left: ^{1}H MAS NMR spectra. Internal projections are shown in dotted lines. The ^{13}C CP MAS NMR spectrum of acetaminophen form I is also given (brown). In panel (a) the dashed lines are used to highlight correlations used for ^{1}H assignment. For clarity, the correlation peaks for the polymer are only highlighted for the polymer's HETCOR in panel (a, black). In panel (b) the dashed lines denotate the carbon signal involved in API-polymer interaction, or API-API interaction for the 40% wt. dispersion while the shaded sections in the spectra mark the cross correlation peaks that shown the API-polymer interactions. Figure SI-8 in the supporting information shown a magnified view of the ^{13}C region at around 110 – 200 ppm, highlighting the API-polymer interactions.

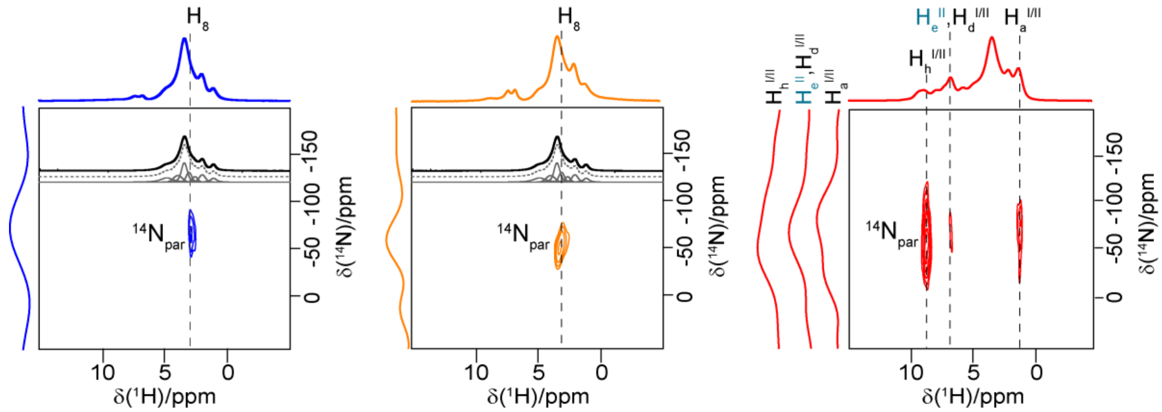

Figure 7. ^{14}N-^{1}H HMQC experiments of 10% wt. (dark blue), 20% wt. (orange) and 40% wt. (red) acetaminophen HPMC-AS ASDs obtained at a MAS frequency of 60 kHz. Data for 10/40% and 20% wt. were collected at 20 T and 18.8 T, respectively. Spectra were recorded with recoupling times of 133.6 µs (10% wt. ASD, 8 rotor periods), 66.8 µs (20 % wt. ASD, 4 rotor periods) and 801.6 µs (40% wt. ASD, 48 rotor periods). The deconvoluted ^{1}H spectra of HPMC-AS under the same condition is also given in black. Spectra on the left of the 2D HMQC are the ^{14}N slices extracted at the indicated ^{1}H chemical shifts in dashed black lines.

detection of the ^{14}N signal in the solid-state represents a challenge. The development of indirectly detected ^{14}N via ^{1}H as for example via 2D ^{14}N-^{1}H HMQC experiments at high magnetic field and very fast MAS frequency has enabled to solve this challenge, establishing this approach as a promising methodology for identifying H-bonding between components in pharmaceutical systems.[51,52,80]. The corresponding ^{14}N-^{1}H HMQC experiments for the 10% wt. and 20% wt. ASDs (Figure 7) identify the presence of correlation between the acetaminophen $^{14}N^{a}$ signal with the -OCH_3 methoxy group (H_8) of the polymer at 3 ppm and highlights H-bonding between this amide donor and oxygen acceptor. In the spectra, no correlation between the NH group of paracetamol and the protons of the substituent groups P, A, and S (Figure 1) were identified, thus excluding the involvement of these groups in the formation of the H-bond between API -polymer.

Importantly, this ^{14}N signal correlating with H_8 does not correspond to same proton (H_h^{a}) identified via ^{15}N CP HECTOR that established the NH correlation within acetaminophen (Figure SI-5) and suggests longer range interactions. We note that this interaction for the 10% wt. and 20% wt. amorphous dispersions was identified using short recoupling times of 133.6 and 66.8 µs, respectively, suggesting a closer contact between acetaminophen and HPMC-AS in those systems than in crystalline acetaminophen, which is consistent with previous work in amorphous formulation.[52] It is proposed that this H-bonding interaction is dominant in order to stabilise acetaminophen in its amorphous form in these ASDs.

In contrast to the 10% wt. and 20% wt. ASDs, the ^{14}N-^{1}H HMQC spectrum for the 40% wt. ASD clearly exhibits correlations between the ^{14}N and ^{1}H ($H_h^{I/II}$, $H_e^{II}/H_d^{I/II}$ and $H_a^{I/II}$) signals within acetaminophen and no correlation to the HPMC-AS polymer, confirming the absence of acetaminophen – HPMC-AS interactions at this high drug loading. The API-API H-bonding interaction was found at significantly longer recoupling times reasonably indicating a longer distance between the packed acetaminophen molecules in the crystal structure when compared the API-polymer distance in amorphous systems as illustrated previously.[50] For both the 10% wt. and 20% wt. amorphous dispersions, the correlation signals in the ^{13}C CP HETCOR experiments carried out at long contact times (Figure 6(b)) and ^{14}N-^{1}H HMQC spectra (Figure 7) highlight intermolecular amorphous drug-polymer H-bonding interactions (Figure 8).

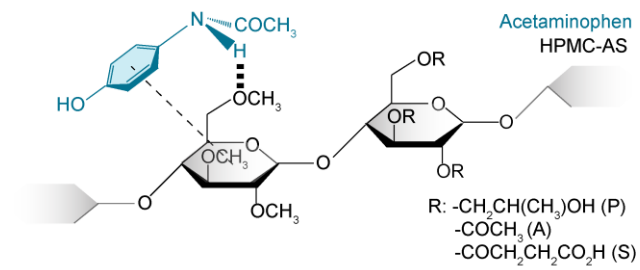

Figure 8. A schematic representation of the interactions that have been experimentally identified in this work. For dispersions with a drug loading of < 20% wt., spatial proximity (---) and H-bond (≡) were identified between the API and the polymer. The acetaminophen and HPMC-AS molecules are given in light blue and black, respectively.

The experimental ^{14}N shifts for the observed signals in Figure 7 and the ^{15}N isotropic chemical shifts obtained in the ^{15}N CP experiments (Figure 5(a)) for the 10% wt. and 20% wt. ASDs are listed in Table 2. The differences in shifts between ^{14}N and ^{15}N are due to the ^{14}N isotropic second-order quadrupolar shift which is given by Eq. 3:

$$\delta_{iso}^{Q}(^{14}N) = \delta_{iso}(^{14}N) - \delta_{iso}(^{15}N) \quad (3)$$

and allows the determination of the quadrupolar product P_Q from Eq. 4:[50]

$$\delta_{iso}^{Q}(^{14}N) = \left(\frac{3}{40}\right)\left(\frac{P_Q}{\nu_0}\right)^2 \times 10^6 \quad (4)$$

where ν_0 is the ^{14}N Larmor frequency. P_Q depends on the quadrupolar coupling constant C_Q and asymmetry parameter η_Q, as expressed by Eq. 5:

$$P_Q = C_Q\sqrt{1+\frac{\eta_Q^2}{3}} \quad (5)$$

Significant difference of around 180-190 ppm between ^{15}N isotropic chemical shift and ^{14}N shift is observed (Table 2) in the acetaminophen HPMC-AS ASD. This is attributed to the isotropic second order quadrupolar shift being sensitive to the presence of the H-bond as previously observed in the 50% wt. acetaminophen-PVP solid dispersion that extracted a $\delta_{iso}^{Q}(^{14}N)$ value of around 184 ppm.[51] This data further supports the presence of acetaminophen HPMC-AS H-bond in the dispersions with drug loading < 20% wt and acetaminophen-acetaminophen H-bond interaction in the recrystallised 40% ASD.

These are stabilising interactions that can be imputed in the understanding of the stability the amorphous acetaminophen – HPMC-AS solid dispersions. Interestingly, the main stabilising interaction that has been identified in this work is H-bonding between the acetaminophen's amide group with the OCH_3 proton (H_8) of the HPMC-AS methyl substituent (M), likely due to the small steric hindrance of this substituent *vs.* the others (Figure 1). This is an unexpected finding given that the acetyl and succinoyl groups in HPMC-AS have been previously suggested to be responsible for the formation of API-polymer H-bonding and contribute to the formation of stabilising interactions.[42]

4. Conclusions

Molecular interactions in acetaminophen – HPMC-AS solid dispersion at 10%, 20% and 40% wt. drug loadings were identified by combining time-dependent PXRD with multidimensional multinuclear NMR experiments. The presence of chemical shift differences in 1D ^{1}H, ^{13}C and ^{15}N CP MAS NMR spectra between crystalline and amorphous acetaminophen suggests a strong structural perturbation in the amorphous species, and can be potentially rationalised by the presence of H-bonding interactions between acetaminophen and the polymer. ^{13}C CP HETCOR exploiting strong ^{13}C-^{1}H dipolar coupling highlighted spatial interaction between the acetaminophen's aromatic protons with the polymer's cellulose ring protons in the 10% wt. and 20% wt. ASDs. This interaction was further unequivocally confirmed by ^{14}N-^{1}H HMQC experiments that identify H-bond interactions between the NH of acetaminophen and the OCH_3 proton of the HPMC-AS methyl substituent. The presence of this type of drug/polymer interaction in amorphous systems is of crucial importance as it stabilises the amorphous dispersions. No acetaminophen - HPMC-AS interactions were found in the 40% wt. dispersion, further validated from ^{1}H relaxation data, indicating the instability of this system and its tendency to recrystallise on a short timescale.

ASSOCIATED CONTENT

Supporting Information

Supporting Information included: acetaminophen and HPMC-AS chemical structures; magnified view of the 190-160 ppm ^{13}C region of the ^{13}C CP spectrum of the recrystallised 40% ASD; residual ^{13}C spectrum between experimental and simulated spectra; ^{13}C CP and HETCOR spectra of the 20% wt. ASD after 1 year at RT/ambient RH; ^{15}N CP HETCOR of the 20% wt. ASD; magnified views of ^{1}H, ^{13}C CP, ^{15}N CP and ^{13}C CP HETCOR spectra; summary of Tg values; tables of ^{1}H and ^{13}C chemical shifts and T_1 relaxation times, ^{1}H $T_{1\rho}$ relaxation times, experimental ^{15}N isotropic chemical shifts $\delta_{iso}(^{15}N)$, ^{14}N shifts $\delta_{iso}(^{14}N)$, ^{14}N quadrupolar-induced shifts δ_{iso}^{Q} and quadrupolar products P_Q for the 20% wt. ASD recorded at 18.8 T.
The Supporting Information is available free of charge on the ACS Publications website.

AUTHOR INFORMATION

Corresponding Author

Frédéric Blanc - Department of Chemistry, University of Liverpool, Crown Street, Liverpool L69 7ZD, United Kingdom; Stephenson Institute for Renewable Energy, University of Liverpool, Peach Street, Liverpool L69 7ZF, United Kingdom; orcid.org/0000-0001-9171-1454;
Email: frederic.blanc@liverpool.ac.uk

Authors

Andrea Pugliese - Department of Chemistry, University of Liverpool, Crown Street, Liverpool L69 7ZD, United Kingdom; orcid.org/0000-0001-7328-0670
Michael Toresco - Rowan College of Engineering, Chemical Engineering Department, Rowan University, Mullica Hill Road, Glassboro, New Jersey 08028, United States;
Daniel McNamara - Drug Product Development, Bristol-Myers Squibb, One Squibb Drive, New Brunswick, New Jersey 08903, United States; orcid.org/0000-0001-5785-2405
Dinu Iuga - Department of Physics, University of Warwick, Gibbet Hill Road, Coventry CV4 7AL, United Kingdom; orcid.org/0000-0001-9315-8250
Anuji Abraham - Drug Product Development, Bristol-Myers Squibb, One Squibb Drive, New Brunswick, New Jersey 08903, United States; orcid.org/0000-0003-3811-7071
Michael Tobyn - Drug Product Development, Bristol-Myers Squibb, Reeds Lane, Moreton CH46 1QW, United Kingdom; orcid.org/0000-0003-0856-7821
Lucy E. Hawarden - Drug Product Development, Bristol-Myers Squibb, Reeds Lane, Moreton CH46 1QW, United Kingdom; orcid.org/0000-0003-1718-4937

Funding Sources

A. P. thanks Bristol-Myers Squibb and EPSRC for a PhD studentship under the scheme of National Productivity Investment Fund (NPIF) (EP/R51231X/1) and F. B. the EPSRC (EP/S013393/1) for funding the 800 MHz spectrometer at the University of Liverpool. The UK 850 MHz solid state NMR Facility used in this research was funded by Engineering and Physical Science Research Council (EPSRC) and Biotechnology and Biological Sciences Research Council (BBSRC) (contract reference PR140003), as well as the University of Warwick including via part funding through the Birmingham Science City Advanced Materials Project 1 and 2 supported by Advantage West

Midlands (AWM) and the European Regional Development Fund (ERDF).

Notes

The authors declare no competing financial interests.

ACKNOWLEDGMENT

A. P. thanks Mr. Robert Clowes (University of Liverpool) for his technical support with the PXRD measurements, Dr. Christopher David and Ms. Danielle Brain (Material Innovation factory – MIF, University of Liverpool) for access to the low temperature freezer, Dr. Ann-Christine Pöppler (University of Würzburg), Dr. Ashlea R. Hughes, and Mr. Benjamin B. Duff (University of Liverpool) for fruitful discussions.

REFERENCES

(1) Amidon, G. L.; Lennernäs, H.; Shah, V. P.; Crison, J. R. A Theoretical Basis for a Biopharmaceutic Drug Classification: The Correlation of in Vitro Drug Product Dissolution and in Vivo Bioavailability. *Pharm. Res.* **1995**, *12*, 413–420.

(2) Rams-Baron, M.; Jachowicz, R.; Boldyreva, E.; Zhou, D.; Jamroz, W.; Paluch, M. *Amorphous Drug*; Springer International Publishing AG: Switzerland, 2018.

(3) Savolainen, M.; Kogermann, K.; Heinz, A.; Aaltonen, J.; Peltonen, L.; Strachan, C.; Yliruusi, J. Better Understanding of Dissolution Behaviour of Amorphous Drugs by in Situ Solid-State Analysis Using Raman Spectroscopy. *Eur. J. Pharm. Biopharm.* **2009**, *71*, 71–79.

(4) *Pharmaceutical Amorphous Solid Dispersion*; Newman, A., Ed.; John Wiley & Sons: Hoboken, New Jersey, 2015.

(5) Leuner, C.; Dressman, J. Improving Drug Solubility for Oral Delivery Using Solid Dispersions. *Eur. J. Pharm. Biopharm.* **2000**, *50*, 47–60.

(6) Van den Mooter, G. The Use of Amorphous Solid Dispersions: A Formulation Strategy to Overcome Poor Solubility and Dissolution Rate. *Drug Discov. Today Technol.* **2012**, *9*, e79–e85.

(7) Baghel, S.; Cathcart, H.; O'Reilly, N. J. Polymeric Amorphous Solid Dispersions: A Review of Amorphization, Crystallization, Stabilization, Solid-State Characterization, and Aqueous Solubilization of Biopharmaceutical Classification System Class II Drugs. *J. Pharm. Sci.* **2016**, *105*, 2527–2544.

(8) Chiou, W. L.; Riegelman, S. Pharmaceutical Applications of Solid Dispersion Systems. *J. Pharm. Sci.* **1971**, *60*, 1281–1302.

(9) Vasconcelos, T.; Marques, S.; das Neves, J.; Sarmento, B. Amorphous Solid Dispersions: Rational Selection of a Manufacturing Process. *Adv. Drug Deliv. Rev.* **2016**, *100*, 85–101.

(10) Singh, A.; Van den Mooter, G. Spray Drying Formulation of Amorphous Solid Dispersions. *Adv. Drug Deliv. Rev.* **2016**, *100*, 27–50.

(11) Wanning, S.; Süverkrüp, R.; Lamprecht, A. Pharmaceutical Spray Freeze Drying. *Int. J. Pharm.* **2015**, *488*, 136–153.

(12) Dong, Z.; Chatterji, A.; Sandhu, H.; Choi, D. S.; Chokshi, H.; Shah, N. Evaluation of Solid State Properties of Solid Dispersions Prepared by Hot-Melt Extrusion and Solvent Co-Precipitation. *Int. J. Pharm.* **2008**, *355*, 141–149.

(13) Law, D.; Schmitt, E. A.; Marsh, K. C.; Everitt, E. A.; Wang, W.; Fort, J. J.; Krill, S. L.; Qiu, Y. Ritonavir Solid Dispersion Qc. *J. Pharm. Sci.* **2004**, *93*, 563–570.

(14) Jones, D. S.; Tian, Y.; Li, S.; Yu, T.; Abu-Diak, O. A.; Andrews, G. P. The Use of Binary Polymeric Networks in Stabilizing Polyethylene Oxide Solid Dispersions. *J. Pharm. Sci.* **2016**, *105*, 3064–3072.

(15) Gupta, P.; Kakumanu, V. K.; Bansal, A. K. Stability and Solubility of Celecoxib-PVP Amorphous Dispersions: A Molecular Perspective. *Pharm. Res.* **2004**, *21*, 1762–1769.

(16) Lehmkemper, K.; Kyeremateng, S. O.; Heinzerling, O.; Degenhardt, M.; Sadowski, G. Long-Term Physical Stability of PVP- and PVPVA-Amorphous Solid Dispersions. *Mol. Pharm.* **2017**, *14*, 157–171.

(17) Dinunzio, J. C.; Hughey, J. R.; Brough, C.; Miller, D. A.; Williams, R. O.; McGinity, J. W. Production of Advanced Solid Dispersions for Enhanced Bioavailability of Itraconazole Using KinetiSol® Dispersing. *Drug Dev. Ind. Pharm.* **2010**, *36*, 1064–1078.

(18) Tanno, F.; Nishiyama, Y.; Kokubo, H.; Obara, S. Evaluation of Hypromellose Acetate Succinate (HPMCAS) as a Carrier in Solid Dispersions. *Drug Dev. Ind. Pharm.* **2004**, *30*, 9–17.

(19) Friesen, D. T.; Shanker, R.; Crew, M.; Smithey, D. T.; Curatolo, W. J.; Nightingale, J. A. S. Hydroxypropyl Methylcellulose Acetate Succinate-Based Spray-Dried Dispersions: An Overview. *Mol. Pharm.* **2008**, *5*, 1003–1019.

(20) Lehmkemper, K.; Kyeremateng, S. O.; Heinzerling, O.; Degenhardt, M.; Sadowski, G. Impact of Polymer Type and Relative Humidity on the Long-Term Physical Stability of Amorphous Solid Dispersions. *Mol. Pharm.* **2017**, *14*, 4374–4386.

(21) Van Duong, T.; Van den Mooter, G. The Role of the Carrier in the Formulation of Pharmaceutical Solid Dispersions. Part II: Amorphous Carriers. *Expert Opin. Drug Deliv.* **2016**, *13*, 1681–1694.

(22) Janssens, S.; Van den Mooter, G. Review: Physical Chemistry of Solid Dispersions. *J. Pharm. Pharmacol.* **2009**, *61*, 1571–1586.

(23) Miller, W. K.; Lyon, D. K.; Friesen, D. T.; Caldwell, W. B.; Vodak, D. T.; Dobry, D. E. Hydroxypropyl Methyl Cellulose Acetate Succinate with Enhanced Acetate and Succinate Substitution. EP2579896A1, 2016.

(24) Qiu, Y.; Chen, Y.; Zhang, G.; Yu, L.; Mantri, R. V. *Developing Solid Oral Dosage Forms - Pharmaceutical Theory and Practice*, 2nd ed.; Elsevier, 2017.

(25) Tobyn, M.; Brown, J.; Dennis, A. B.; Fakes, M.; Gao, Q.; Gamble, J.; Khimyak, Y. Z.; McGeorge, G.; Patel, C.; Sinclair, W.; Timmins, P.; Yin, S. Amorphous Drug–PVP Dispersions: Application of Theoretical, Thermal and Spectroscopic Analytical Techniques to the Study of a Molecule With Intermolecular Bonds in Both the Crystalline and Pure Amorphous State. *J. Pharm. Sci.* **2009**, *98*, 3456–3468.

(26) McNamara, D.; Yin, S.; Pan, D.; Crull, G.; Timmins, P.; Vig, B. Characterization of Phase Separation Propensity for Amorphous Spray Dried Dispersions. *Mol. Pharm.* **2017**, *14*, 377–385.

(27) De Villiers, M. M.; Wurster, D. E.; Van Der Watt, J. G.; Ketkar, A. X-Ray Powder Diffraction Determination of the Relative Amount of Crystalline Acetaminophen in Solid Dispersions with Polyvinylpyrrolidone. *Int. J. Pharm.* **1998**, *163*, 219–224.

(28) Baird, J. A.; Taylor, L. S. Evaluation of Amorphous Solid Dispersion Properties Using Thermal Analysis Techniques. *Adv. Drug Deliv. Rev.* **2012**, *64*, 396–421.

(29) Smith, G.; Hussain, A.; Bukhari, N. I.; Ermolina, I. Quantification of Residual Crystallinity in Ball Milled Commercially Sourced Lactose Monohydrate by Thermo-Analytical Techniques and Terahertz Spectroscopy. *Eur. J. Pharm. Biopharm.* **2015**, *92*, 180–191.

(30) Mooter, G. Van Den; Brande, J. Van Den; Augustijns, P.; Kinget, R. Glass Forming Properties of Benzodiazepines and Co-Evaporate Systems with Poly (Hydroxyethyl Methacrylate). *J. Therm. Anal.* **1999**, *57*, 493–507.

(31) Paudel, A.; Van Humbeeck, J.; Van den Mooter, G. Theoretical and Experimental Investigation on the Solid Solubility and Miscibility of Naproxen in Poly(Vinylpyrrolidone). *Mol. Pharm.* **2010**, *7*, 1133–1148.

(32) Gordon, M.; Taylor, J. S. Ideal Copolymers and the Second-Order Transitions of Synthetic Rubbers. I. Noncrystalline Copolymers. *Rubber Chem. Technol.* **1953**, *26*, 323–335.

(33) Lehmkemper, K.; Kyeremateng, S. O.; Bartels, M.; Degenhardt, M.; Sadowski, G. Physical Stability of API/Polymer-Blend Amorphous Solid Dispersions. *Eur. J. Pharm. Biopharm.* **2018**, *124*, 147–157.

(34) Tres, F.; Patient, J. D.; Williams, P. M.; Treacher, K.; Booth, J.; Hughes, L. P.; Wren, S. A. C.; Aylott, J. W.; Burley, J. C. Monitoring the Dissolution Mechanisms of Amorphous Bicalutamide Solid Dispersions via Real-Time Raman Mapping. *Mol. Pharm.* **2015**, *12*, 1512–1522.

(35) Furuyama, N.; Hasegawa, S.; Hamaura, T.; Yada, S.; Nakagami, H.; Yonemochi, E.; Terada, K. Evaluation of Solid Dispersions on a Molecular Level by the Raman Mapping Technique. *Int. J. Pharm.* **2008**, *361*, 12–18.

(36) Taylor, L. S.; Zografi, G. Spectroscopic Characterization of Interactions Between PVP and Indomethacin in Amorphous Molecular Dispersions. *Pharm. Res.* **1997**, *14*, 1691–1698.

(37) Tran, T. T. D.; Tran, P. H. L. Molecular Interactions in Solid Dispersions of Poorly Water-Soluble Drugs. *Pharmaceutics* **2020**, *12*, 1–12.

(38) Asnaini. *NMR Spectroscopy in Pharmaceutical Analysis*; U. Holzgrabe, U., Wawer, I., Diehl, B., Eds.; Elsevier Science, Oxford 2008., 2008.

(39) *NMR in Pharmaceutical Science*; Everett, J. R., Harris, R. K., Lindon, J. C., Wilson, I. D., Eds.; Wilson Wiley, 2015.

(40) Pellecchia, M.; Bertini, I.; Cowburn, D.; Dalvit, C.; Giralt, E.; Jahnke, W.; James, T. L.; Homans, S. W.; Kessler, H.; Luchinat, C.; Meyer, B.; Oschkinat, H.; Peng, J.; Schwalbe, H.; Siegal, G. Perspectives on NMR in Drug Discovery: A Technique Comes of Age. *Nat. Rev. Drug Discov.* **2008**, *7*, 738–745.

(41) Sperger, D. M.; Munson, E. J. Analysis of Structural Variability in Pharmaceutical Excipients Using Solid-State NMR Spectroscopy. *AAPS PharmSciTech* **2011**, *12*, 821–833.

(42) Ishizuka, Y.; Ueda, K.; Okada, H.; Takeda, J.; Karashima, M.; Yazawa, K.; Higashi, K.; Kawakami, K.; Ikeda, Y.; Moribe, K. Effect of Drug–Polymer Interactions through Hypromellose Acetate Succinate Substituents on the Physical Stability on Solid Dispersions Studied by Fourier-Transform Infrared and Solid-State Nuclear Magnetic Resonance. *Mol. Pharm.* **2019**, *16*, 2785–2794.

(43) Paudel, A.; Geppi, M.; Van Den Mooter, G. Structural and Dynamic Properties of Amorphous Solid Dispersions: The Role of Solid-State Nuclear Magnetic Resonance Spectroscopy and Relaxometry. *J. Pharm. Sci.* **2014**, *103*, 2635–2662.

(44) Lu, X.; Huang, C.; Lowinger, M. B.; Yang, F.; Xu, W.; Brown, C. D.; Hesk, D.; Koynov, A.; Schenck, L.; Su, Y. Molecular Interactions in Posaconazole Amorphous Solid Dispersions from Two-Dimensional Solid-State NMR Spectroscopy. *Mol. Pharm.* **2019**, *16*, 2579–2589.

(45) Li, M.; Meng, F.; Tsutsumi, Y.; Amoureux, J. P.; Xu, W.; Lu, X.; Zhang, F.; Su, Y. Understanding Molecular Interactions in Rafoxanide-Povidone Amorphous Solid Dispersions from Ultrafast Magic Angle Spinning NMR. *Mol. Pharm.* **2020**, *17*, 2196–2207.

(46) Struppe, J.; Quinn, C. M.; Sarkar, S.; Gronenborn, A. M.; Polenova, T. Ultrafast ^{1}H MAS NMR Crystallography for Natural Abundance Pharmaceutical Compounds. *Mol. Pharm.* **2020**, *17*, 674–682.

(47) Hirsh, D. A.; Wijesekara, A. V.; Carnahan, S. L.; Hung, I.; Lubach, J. W.; Nagapudi, K.; Rossini, A. J. Rapid Characterization of Formulated Pharmaceuticals Using Fast MAS ^{1}H Solid-State NMR Spectroscopy. *Mol. Pharm.* **2019**, *16*, 3121–3132.

(48) Gan, Z.; Paul, J.; Tre, J. Proton-Detected N MAS NMR Using Homonuclear Decoupled Rotary Resonance. *Chem. Physcs Lett.* **2007**, *435*, 163–169.

(49) Tatton, A. S.; Pham, T. N.; Vogt, F. G.; Iuga, D.; Edwards, A. J.; Brown, S. P. Probing Intermolecular Interactions and Nitrogen Protonation in Pharmaceuticals by Novel ^{15}N-Edited and 2D ^{14}N-^{1}H Solid-State NMR. *CrystEngComm* **2012**, *14*, 2654–2659.

(50) Tatton, A. S.; Bradley, J. P.; Iuga, D.; Brown, S. P. ^{14}N-^{1}H Heteronuclear Multiple-Quantum Correlation Magic-Angle Spinning NMR Spectroscopy of Organic Solids. *Z. Phys. Chem.* **2012**, *226*, 1187–1203.

(51) Tatton, A. S.; Pham, T. N.; Vogt, F. G.; Iuga, D.; Edwards, A. J.; Brown, S. P. Probing Hydrogen Bonding in Cocrystals and Amorphous Dispersions Using ^{14}N – ^{1}H HMQC Solid-State NMR. *Mol. Pharm.* **2013**, *10*, 999–1007.

(52) Grüne, M.; Luxenhofer, R.; Iuga, D.; Brown, S. P.; Pöppler, A. C. ^{14}N-^{1}H HMQC Solid-State NMR as a Powerful Tool to Study Amorphous Formulations-an Exemplary Study of Paclitaxel Loaded Polymer Micelles. *J. Mater. Chem. B* **2020**, *8*, 6827–6836.

(53) Druzhbin, D. A.; Drebushchak, T. N.; Min'kov, V. S.; Boldyreva, E. V. Crystal Structure of Two Paracetamol Polymorphs at 20 K: A Search for the "Structure- Property" Relationship. *J. Struct. Chem.* **2015**, *56*, 317–323.

(54) Nguyen Thi, Y.; Rademann, K.; Emmerling, F. Direct Evidence of Polyamorphism in Paracetamol. *CrystEngComm* **2015**, *17*, 9029–9036.

(55) Pisa, E.; Hughes, L. P.; Wren, S. A. C.; Booth, J.; McCabe, J. F.; Whittaker, D. T. E.; Mantle, M. D. NMR and Thermal Studies for the Characterization of Mass Transport and Phase Separation in Paracetamol/Copovidone Hot-Melt Extrusion Formulations. *Mol. Pharm.* **2020**, *17*, 2021–2033.

(56) Bräuniger, T.; Wormald, P.; Hodgkinson, P. Improved Proton Decoupling in NMR Spectroscopy of Crystalline Solids Using the SPINAL-64 Sequence. *Monatshefte fur Chemie / Chem. Mon.* **2002**, *133*, 1549–1554.

(57) Hartmann, S. R.; Hahn, E. L. Nuclear Double Resonance in the Rotating Frame. *Phys. Rev.* **1962**, *128*, 2042–2053.

(58) Van Rossum, B. J.; Förster, H.; De Groot, H. J. M. High-Field and High-Speed CP-MAS ^{13}C NMR Heteronuclear Dipolar-Correlation Spectroscopy of Solids with Frequency-Switched Lee-Goldburg Homonuclear Decoupling. *J. Magn. Reson.* **1997**, *124*, 516–519.

(59) Oas, T. G.; Griffin, R. G.; Levitt, M. H. Rotary Resonance Recoupling of Dipolar Interactions in Solid - State Nuclear Magnetic Resonance Spectroscopy. *J. Chem. Phys.* **1988**, *692*, 692–695.

(60) Costa, P. R.; Gross, J. D.; Hong, M.; Griffin, R. G. Solid-State NMR Measurement of Ψ in Peptides: A NCCN 2Q-Heteronuclear Local Field Experiment. *Chem. Phys. Lett.* **1997**, *280*, 95–103.

(61) Morcombe, C. R.; Zilm, K. W. Chemical Shift Referencing in MAS Solid State NMR. *J. Magn. Reson.* **2003**, *162*, 479–486.

(62) Bertani, P.; Raya, J.; Bechinger, B. ^{15}N Chemical Shift Referencing in Solid State NMR. *Solid State Nucl. Magn. Reson.* **2014**, *61–62*, 15–18.

(63) Jakobsen, H. J.; Hove, A. R.; Hazell, R. G.; Bildsøe, H.; Skibsted, J. Solid-State ^{14}N MAS NMR of Ammonium Ions as a Spy to Structural Insights for Ammonium Salts. *Magn. Reson. Chem.* **2006**, *44*, 348–356.

(64) Perrin, M. A.; Neumann, M. A.; Elmaleh, H.; Zaske, L. Crystal Structure Determination of the Elusive Paracetamol Form III. *Chem. Commun.* **2009**, No. 22, 3181.

(65) Telford, R.; Seaton, C. C.; Clout, A.; Buanz, A.; Gaisford, S.; Williams, G. R.; Prior, T. J.; Okoye, C. H.; Munshi, T.; Scowen, I. J. Stabilisation of Metastable Polymorphs: The Case of Paracetamol Form III. *Chem. Commun.* **2016**, *52*, 12028–12031.

(66) Li, Y.; Pang, H.; Guo, Z.; Lin, L.; Dong, Y.; Li, G.; Lu, M.; Wu, C. Interactions between Drugs and Polymers Influencing Hot Melt Extrusion. *J. Pharm. Pharmacol.* **2014**, *66*, 148–166.

(67) Maldonado-Santoyo, M.; Nuño-Donlucas, S. M.; Cesteros, L. C.; Katime, I. Miscibility and Specific Interactions in Blends of Poly(Vinyl Phenyl Ketone Hydrogenated) with Poly(2,6-Dimethyl-1,4-Phenylene Oxide). *J. Appl. Polym. Sci.* **2004**, *91*, 1887–1892.

(68) Burley, J. C.; Duer, M. J.; Stein, R. S.; Vrcelj, R. M. Enforcing Ostwald's Rule of Stages: Isolation of Paracetamol Forms III and II. *Eur. J. Pharm. Sci.* **2007**, *31*, 271–276.

(69) Pugliese, A.; Hawarden, L. E.; Abraham, A.; Tobyn, M.; Blanc, F. Solid State Nuclear Magnetic Resonance Studies of Hydroxypropylmethylcellulose Acetyl Succinate Polymer, a Useful Carrier in Pharmaceutical Solid Dispersions. *Magn. Reson. Chem.* **2020**, *58*, 1036–1048.

(70) Hodgkinson, P. NMR Crystallography of Molecular Organics. *Prog. Nucl. Magn. Reson. Spectrosc.* **2020**, *118*, 10–53.

(71) Lu, X.; Xu, W.; Hanada, M.; Jermain, S. V.; Williams, R. O.; Su, Y. Solid-State NMR Analysis of Crystalline and Amorphous Indomethacin: An Experimental Protocol for Full Resonance Assignments. *J. Pharm. Biomed. Anal.* **2019**, *165*, 47–55.

(72) Yuan, X.; Xiang, T. X.; Anderson, B. D.; Munson, E. J. Hydrogen Bonding Interactions in Amorphous Indomethacin and Its Amorphous Solid Dispersions with Poly(Vinylpyrrolidone) and Poly(Vinylpyrrolidone-Co-Vinyl Acetate) Studied Using ^{13}C Solid-State NMR. *Mol. Pharm.* **2015**, *12*, 4518–4528.

(73) Nie, H.; Su, Y.; Zhang, M.; Song, Y.; Leone, A.; Taylor, L. S.; Marsac, P. J.; Li, T.; Byrn, S. R. Solid-State Spectroscopic Investigation of Molecular Interactions between Clofazimine and Hypromellose Phthalate in Amorphous Solid Dispersions. *Mol. Pharm.* **2016**, *13*, 3964–3975.

(74) Song, Y.; Yang, X.; Chen, X.; Nie, H.; Byrn, S.; Lubach, J. W. Investigation of Drug-Excipient Interactions in Lapatinib Amorphous Solid Dispersions Using Solid-State NMR Spectroscopy. *Mol. Pharm.* **2015**, *12*, 857–866.

(75) Duan, P.; Lamm, M. S.; Yang, F.; Xu, W.; Skomski, D.; Su, Y.; Schmidt-Rohr, K. Quantifying Molecular Mixing and Heterogeneity in Pharmaceutical Dispersions at Sub-100 Nm Resolution by Spin Diffusion NMR. *Mol. Pharm.* **2020**, *17*, 3567–3580.

(76) Pham, T. N.; Watson, S. J.; Edwards, A. J.; Chavda, M.; Clawson, J. S.; Strohmeier, M.; Vogt, F. G. Analysis of Amorphous Solid Dispersions Using 2D Solid-State NMR and 1H T1 Relaxation Measurements. *Mol. Pharm.* **2010**, *7*, 1667–1691.

(77) Dickinson, L. C.; Yang, H.; Chu, C. W.; Stein, R. S.; Chien, J. C. W. Limits to Compatibility in Poly(x-Methylstyrene)/Poly(2,6-Dimethylphenylene Oxide) Blends by NMR. *Macromolecules* **1987**, *20*, 1757–1760.

(78) Bovey, F. A.; Mirau, P. A. *NMR of Polymers*, 1st ed.; Academic Press: San Diego, CA, 1996.

(79) Yuan, X.; Sperger, D.; Munson, E. J. Investigating Miscibility and Molecular Mobility of Nifedipine-PVP Amorphous Solid Dispersions Using Solid-State NMR Spectroscopy. *Mol. Pharm.* **2014**, *11*, 329–337.

(80) Maruyoshi, K.; Iuga, D.; Antzutkin, O. N.; Alhalaweh, A.; Velaga, S. P.; Brown, S. P. Identifying the Intermolecular Hydrogen-Bonding Supramolecular Synthons in an Indomethacin – Nicotinamide Cocrystal by Solid-State NMR. *Chem. Commun.* **2012**, *48*, 10844–10846.

TOC

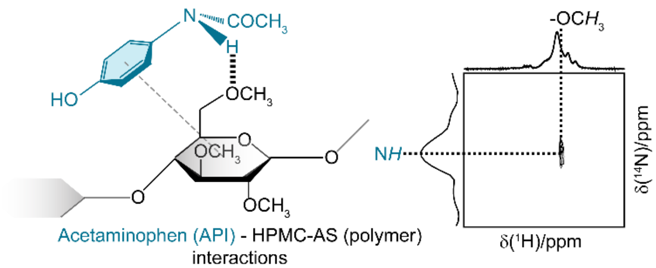

-OCH3
N
COCH3
H
HO
OCH3
OCH3
O
O
O
OCH3
NH
δ(14N)/ppm
δ(1H)/ppm
Acetaminophen (API) - HPMC-AS (polymer) interactions